Luminescence from laser-created bubbles in cryogenic liquids

Ohan Baghdassarian, Bernd Tabbert, and Gary A. Williams
Department of Physics and Astronomy, University of California, Los Angeles, California 90095, USA
(Received 5 January 2007; published 6 June 2007)

A luminescence pulse is observed from laser-created bubbles in pressurized liquid nitrogen and argon, occurring at the first collapse point of the bubble motion. The duration of the light pulse depends linearly on the bubble size, ranging from 200 ns to 1 μs for bubbles with maximum diameters between 0.2 and 1 mm. The spectrum of the light consists entirely of atomic lines, which surprisingly turns out to contain strong emission lines from excited states of the neutral chromium atom. It is likely that this results from small microflakes of stainless steel knocked off the walls of the sample cell by the shock waves generated from the laser pulse. The small metallic flakes are preferentially ionized by the laser, resulting in bubbles containing chromium and other metal atoms in their interior. An analysis of the relative intensities of the triplet chromium lines shows that the compression in the bubble collapse is heating the chromium to temperatures of order 4500 K.

DOI: 10.1103/PhysRevE.75.066305 PACS number(s): 78.60.Mq, 47.55.dd, 61.25.Bi, 52.50.Lp

I. INTRODUCTION

Luminescence from collapsing bubbles in water has been previously studied in a variety of different experimental configurations, including single- and multi-bubble sonoluminescence [1], laser-created bubbles [2–4], Venturi-tube flows [5], and shake-table water hammers [6]. Despite all of this effort, however, the mechanism of the light emission is still not well-understood. A consensus has emerged that the strong adiabatic heating of the gas inside the bubble during the rapid collapse of the bubble wall is the key feature leading to the light emission, but the details of the process remain unclear. There is, for example, still no theoretical explanation for the observation with laser-created bubbles in water that the duration of the luminescence pulse is linear in the maximum bubble size [3] and increases when external pressure is applied to the system [7]. The degree of plasma formation in the heated gas also remains poorly understood; the observation of a spectrum similar to that of a black body in collapsing water bubbles [4] implies that the photon mean free path must be smaller than the hot-spot size of tens of micrometers, something impossible to achieve in ordinary laboratory plasmas. The difficulty in formulating a consistent theory of the luminescence dynamics is the extreme spatial and temporal variation of the pressure, density, and temperature inside the bubble. The atomic density of the gas in the bubble can vary from $10^{16}/\mathrm{cm}^3$ at the maximum bubble radius to $10^{23}/\mathrm{cm}^3$ at the collapse point, with most of the change occurring on a time scale of a few hundred nanoseconds.

To gain a better understanding of the luminescence it is necessary to expand the parameter space of different liquids where the phenomenon can be observed. Since there were early reports in the literature that luminescence could be observed from bubbles in liquid nitrogen [8,9], we initially undertook an investigation of whether single-bubble sonoluminescence could be observed in cryogenic liquids. It proved to be possible to acoustically trap helium and neon bubbles in liquid nitrogen [10], and the bubble dynamics (monitored by laser Mie scattering) were quite interesting [11]. However, we were never able to observe any sonoluminescence from these bubbles, since as the driving sound field was increased the bubble trapping would suddenly be lost. This occurred for expansion ratios (maximum radius to ambient radius) of about 10, which for water is just about where sonoluminescence begins, but for the cryogenic liquids this is apparently not quite enough drive amplitude. We speculate that the bubble loss occurs due to the onset of instabilities of the bubble surface wave modes, which will occur for lower drives than in water, since the surface tension of the cryogenic liquids is 6 to 7 times smaller than water.

With single-bubble sonoluminescence not being possible in the cryogenic liquids, we turned instead to the laser-creation technique using a high-intensity pulsed laser beam focused into the fluids [12], and this proved to be successful in producing a luminescence pulse [13]. The luminescence observed at the bubble collapse point in both liquid nitrogen and liquid argon is surprisingly quite different than for laser-created bubbles in water. The pulse duration is found to be about 100 times longer than for bubbles of the same maximum radius in water, though in both cases it increases linearly with the maximum radius. The spectrum of the luminescence consists entirely of atomic lines, unlike the continuous blackbody spectrum seen for water bubbles [4]. A major surprise was the fact that two of the strongest lines in the spectrum could be identified as arising from chromium atoms that are being heated to temperatures of 4500 K in the bubble collapse. We believe that this observation is due to small flakes of stainless steel floating in the cryogenic liquid that are subsequently ionized by the focused laser pulse. The flakes are probably knocked off the walls of the experimental cell by the shock waves generated by the laser pulse.

II. APPARATUS

The sample cell is machined out of type 304 stainless steel, a cylinder of inner diameter 3.4 cm and length 10 cm, with flanges on each end for making indium O-ring seals. The surface of the cell was anodized black with a "hot black oxide" (Fe_3O_4) plating in order to minimize optical reflec-

tions. Four window ports are mounted at the center to provide optical access, with quartz windows 3 mm thick and 19 mm diameter sealed with indium O-rings on three of the windows, while a quartz lens with focal length 2 cm is mounted on the fourth port. This cell could be pressurized up to 30 bars through a 3 mm diameter stainless steel tube connected to the room-temperature part of the apparatus. Cryogenic liquids were condensed into the cell through this tube using high-purity (99.999%) gases.

The cell is suspended in a custom vari-temp optical dewar [14]. A reservoir of liquid nitrogen in the dewar is pumped through a variable capillary, and this provides cooling for a chamber surrounding the cell, which is cooled by a few torr of helium gas in the chamber. The temperature is primarily controlled by regulating the vapor pressure of the pumped liquid nitrogen, and secondarily by a feedback heater epoxied to the cell that is controlled by the output of a diode thermometer also mounted on the cell. With this system the cell temperature could easily be varied over the range between 66 and 100 K needed for investigating liquid nitrogen, argon, and oxygen, with a temperature stability of order 0.1 K. Typically the operating temperature was chosen to be as low as possible without solidification, in order to minimize the vapor pressure in the bubble, which can affect the bubble dynamics. In liquid nitrogen, for example, the minimum possible vapor pressure is about 0.16 bar at 65 K.

The bubbles are created by focusing 5 ns pulses from a neodium: yttrium aluminum garnet (YAG) laser at 1064 nm into the center of the cell, ionizing the cryogenic liquid over a region estimated to be 10 μm in diameter. The laser energy is slowly increased to the fairly sharp threshold value where the ionization is induced on every laser shot, estimated to be about 0.1 to 0.2 J focused into the liquid. The plasma that is created quickly recombines over 50–100 ns, but the energy absorbed from the laser pulse then appears as the kinetic energy of an expanding bubble. The radius of the bubble is monitored by backlighting the bubble with either a 1 W diode laser at 974 nm or a 100 mW argon ion laser at 488 nm and detecting the postbubble beam intensity with a photodiode. The bubble refracts light out of the beam proportional to the bubble area, and hence taking the square root gives a signal proportional to the bubble radius. This can be calibrated from the observed time T_c to the first collapse point of the bubble motion, since it is related to the maximum radius R_m by the Raleigh formula

$$R_m = 0.55\sqrt{\frac{p - p_v}{\rho}}T_c, \tag{1}$$

with p the applied pressure, ρ the liquid density, and p_v the vapor pressure at the operating temperature (which can be appreciable for these cryogenic liquids). The bubbles can be photographed by replacing the photodiode with a long-distance microscope and charge coupled device (CCD) camera combination, and pulsing the backlighting laser on for times of order 0.1–0.5 μs at a specified point in the bubble motion.

The luminescence at the bubble collapse point is monitored with a photomultiplier, a Hamamtsu model R2027 with about a 3 ns risetime, with sensitivity between 200 and 800 nm. For the spectrum measurements the light is focused onto the entrance slit of a 0.3 m spectrometer using paraboloidal mirrors, and an intensified CCD detector allows collection of a wide spectral range with each bubble collapse. The integration on the CCD is triggered by the rising edge of the luminescence pulse. A 300 lines/mm grating in the spectrometer and a 1 mm slit gives a spectral range of 200 nm with resolution of about 2 nm, while a 1200 lines/mm grating gives 30 nm with a resolution of 0.3 nm. Typically the luminescence from 15 to 20 bubbles with nearly the same maximum radius is averaged for each wavelength range, and the data is then matched in the regions where the wavelength ranges overlap. The wavelength scale of the spectrometer is calibrated in the blue using a mercury-argon lamp with an accuracy of about 1 nm, while the detection efficiency of the spectrometer and the collecting optics is calibrated using a deuterium lamp in the blue and a quartz-halogen lamp in the infrared.

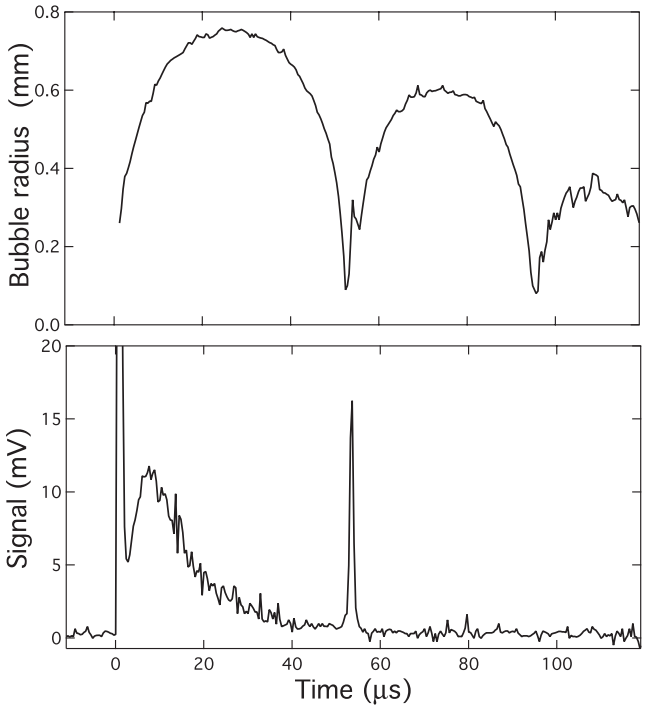

FIG. 1. Liquid nitrogen at $T=66.0$ K, $p=5.8$ bar: bubble radius and light emission detected by the photomultiplier as a function of time from the laser pulse at $t=0$.

III. RESULTS

Figure 1 shows a bubble created in liquid nitrogen at 66.0 K and pressurized to 5.8 bar. The laser-induced ionization flash at $t=0$ leads to an expanding bubble which reaches a maximum radius of 0.75 mm and also to an initial luminescence signal that reaches a peak at about 10 μs and then decays away after 50 μs. This initial luminescence, very similar to that also seen with laser-created bubbles in water [3] probably arises from metastable atomic or molecular states created either in the recombination following the ion-

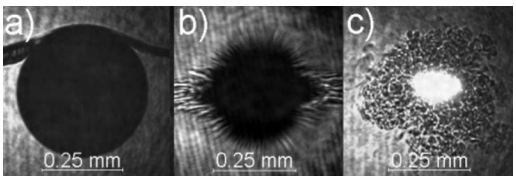

FIG. 2. Photographs of bubbles in liquid nitrogen at 66.0 K and 5.8 bars: (a) $t=4$ μs from the YAG pulse, (b) $t=45$ μs just before the first collapse, and (c) $t=90$ μs near the second collapse point (the bright spot is the backlighting laser).

ization, or created by the uv emission into the liquid surrounding the ionization region. The main luminescence signal of interest in this paper is the sharp luminescence pulse seen at the first collapse point of the bubble at $t=53$ μs. The rebound of the bubble past this point is quite large when compared to the similar case in water, where the second "bounce" is often only a small fraction of the initial maximum radius [3]. Similar large "afterbounces" were also observed in liquid nitrogen bubbles driven by a strong acoustic field [11].

Photographs of the bubbles in liquid nitrogen at 66 K and 5.8 bar are shown in Fig. 2. Figure 2(a) shows an expanding bubble 4 μs after it was created, pushing the heated plume from the focused YAG laser ahead of it. The plume is visible because the reduced density from the heating changes the refractive index and scatters the backlight. Figure 2(b) shows a collapsing bubble at $t=45$ μs, close to the first minimum radius. The convection tendrils streaming away from the bubble show that there must be some conduction of the compressional heating into the surrounding liquid. In Fig. 2(c) taken close to the second collapse minimum at $t=90$ μs the bubble surface is not readily visible; the heating tendrils appear to dominate.

It was found necessary to pressurize the liquid to more than a few bars before the sharp collapse luminescence could be observed, and even then there was considerable variation from shot to shot in the magnitude of the luminescence pulse and in the maximum radius of the bubble (similar effects are seen in water [3,4,7], and are thought to be due to differing sizes of the impurities floating in the liquid that absorb the initial laser energy and induce the subsequent ionization). When the pressure on the liquid nitrogen is reduced to 1 bar or less the collapse luminescence is never observed, but on many shots an unusual effect is seen with the metastable luminescence, shown in Fig. 3(a). The luminescence abruptly decreases to some fraction of its value at the time corresponding to the first bubble collapse point, and then continues to slowly decay. This is probably connected with the metastable species that are created both inside the bubble and in the liquid surrounding the bubble at the time of the laser ionization. Near the collapse point the metastables inside the bubble will experience a very rapid change in density and temperature, leading to transitions to the ground state without visible radiation, while the metastables outside the bubble will be unaffected and continue to decay radiatively. When the pressure is increased above 1 bar the signal from metastables inside the bubble decreases, and in a number of laser shots disappears completely. Between 2 and 3 bars the

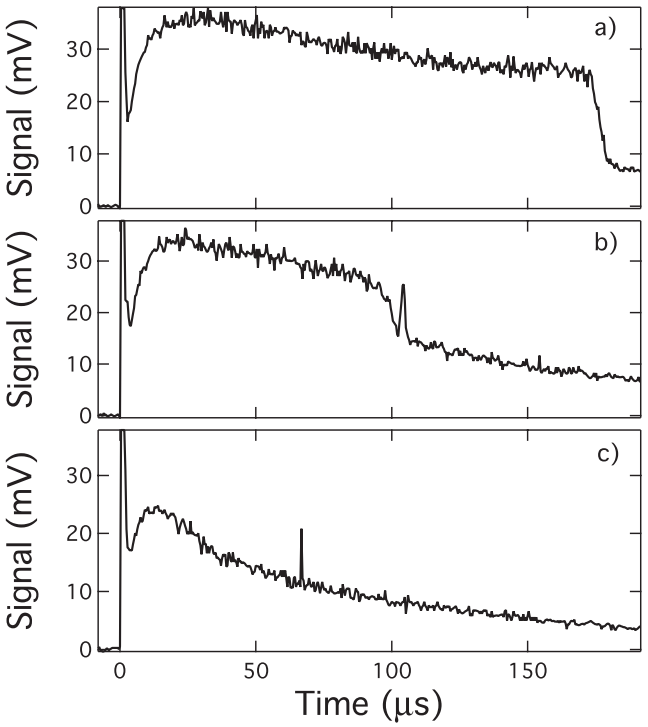

FIG. 3. Liquid nitrogen at $T=66.0$ K: photomultiplier signal versus time from the laser pulse at $t=0$, at pressures (a) 1 bar, (b) 3 bars, and (c) 3 bars.

sharp collapse luminescence starts to become visible on some shots. Figure 3(b) shows a shot at 3 bars where both the metastable signal inside the bubble and the sharp collapse luminescence are both visible. Figure 3(c), also at 3 bars, shows a shot where only the metastables outside the bubble contribute to the light signal, where they are not affected by the collapse, marked by the sharp luminescence. At 5 bars and above most of the shots took the form shown in Fig. 1, though occasionally signals like those of Fig. 3(b) were still seen.

Figure 4 shows a photograph of the luminescence spot, taken using the intensified CCD coupled to the long distance microscope. Superimposed is an image of the rebounding bubble several μs past the collapse point taken by a 100 ns pulse of the backlighting argon laser. Horizontal and vertical scans of the optical intensity through the center of the luminescence spot are shown above the photograph. The luminescence appears to be uniformly distributed, with a diameter at half maximum intensity of about 70 μm. We have not attempted to make any corrections for the distortion due to the refractive index of the liquid nitrogen and the curved bubble wall, since the wall position right at the collapse point is not determined in this measurement.

The luminescence signal at the collapse point is shown on an expanded time scale in Fig. 5 for a bubble in liquid nitrogen at 6 bars with $R_m=0.53$ mm. The surprising feature here is the long duration of the pulse, with a full width at half maximum of 560 ns. This is about 100 times longer than would be observed for the luminescence pulse of a similar laser-created bubble in water [3,7]. Figure 6 shows the pulse width as a function of bubble size, and on average the width

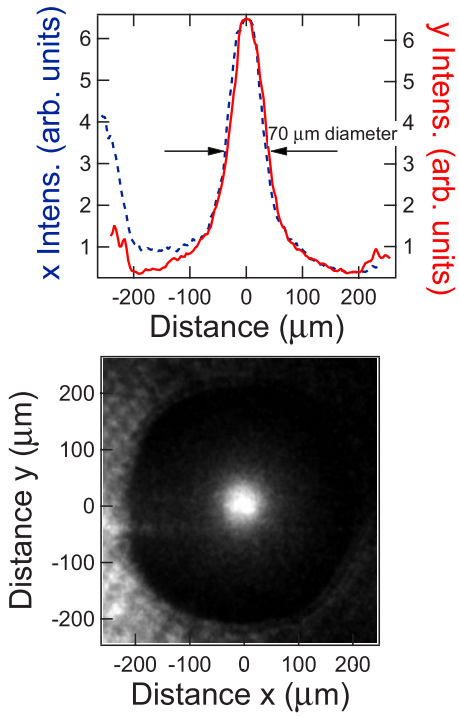

FIG. 4. (Color online) Photograph of the luminescence spot in the bubble, superimposed on an image of the bubble just on the rebound. The upper curves are scans across the image of the optical intensity in the horizontal x direction at $y=0$ (dashed line) and vertical y direction at $x=0$ (solid line).

is directly proportional to the bubble size. This behavior is entirely similar to that seen in water [3,7], though now with a slope 100 times larger. We checked to see if the time dependence of the spectral components of the pulse had any variation by using various red and blue filters to block the different components on two photomultipliers viewing the same pulse, but no differences in the pulse shape could be detected, to within the resolution of several nanoseconds. The number of photons in the pulse can be determined by calibrating the photon sensitivity of the photomultiplier by

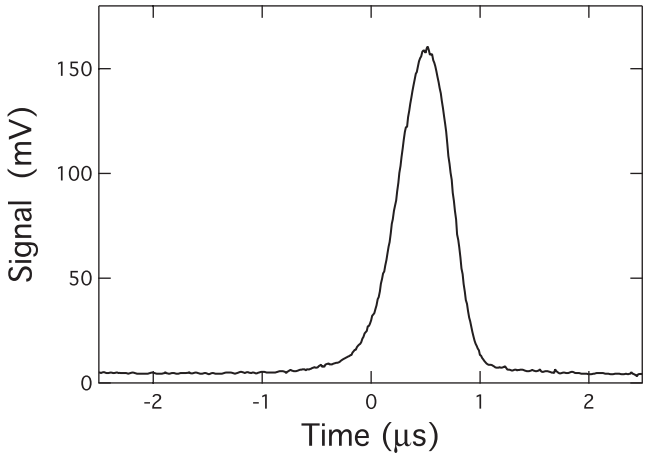

FIG. 5. Sharp collapse luminescence on an expanded time scale in liquid nitrogen, $T=65.6$ K, $p=6$ bar, $T_c=36.0$ μs, and $R_m=0.53$ mm.

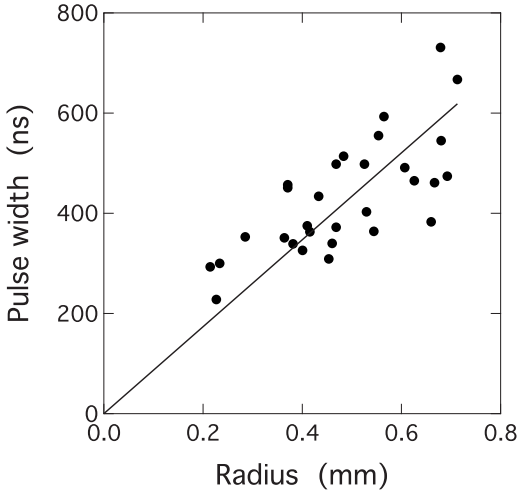

FIG. 6. Pulse width (full width at half maximum) as a function of the maximum bubble radius in liquid nitrogen, $T=66.0$ K, $p=5.8$ bar. The solid line is a linear fit to the data, assuming a zero intercept.

integrating single-electron dark-current pulses, and dividing by the quantum efficiency of the photocathode and the fractional solid angle subtended by the detector face. Integrating the luminescence pulses gives about 10^{10} photons for a bubble of maximum radius 1 mm. This is about 100 times the number of photons observed from a similar bubble in water [3]. The difference here probably results from the fact that the emission time is about 100 times longer than in water.

Very similar collapse luminescence pulses were observed for laser-created bubbles in liquid argon, at temperatures around 84 K. It was again found necessary to pressurize to a few bars before the luminescence appeared. When experiments were carried out with liquid oxygen condensed into the cell at temperatures between 66 and 77 K, however, no collapse luminescence at all could be observed, even at pressures up to 10–12 bars. Bubbles were certainly being generated, and the radius-time curves looked very similar to those in liquid nitrogen, but no luminescence pulses were apparent. Liquid helium was also tried on one run, at temperatures down to 1.5 K and pressures to 25 bar, but the bubbles created by the laser were quite large (4–8 mm) and became unstable even during the initial expansion, and again no luminescence could be observed. The threshold laser energy for ionization of the liquid was found to be similar to that of the other cryogenic liquids, but since the latent heat of helium is much smaller than those liquids, a much larger volume of the liquid will be vaporized, leading to the large bubbles. It may be possible to get smaller bubbles using a picosecond laser where less total energy would be absorbed, but we were unable to try this.

The spectrum of the collapse luminescence is shown in Fig. 7 for both liquid nitrogen ($T=66$ K, $p=4$ bar) and liquid argon ($T=84$ K, $p=4.5$ bar). Only atomic lines are observed, indicating that the plasma created in the bubble interior must be optically thin, compared with the smooth blackbody-like spectra observed in water [4,7]. It was initially very puzzling, however, that none of these lines matched the known

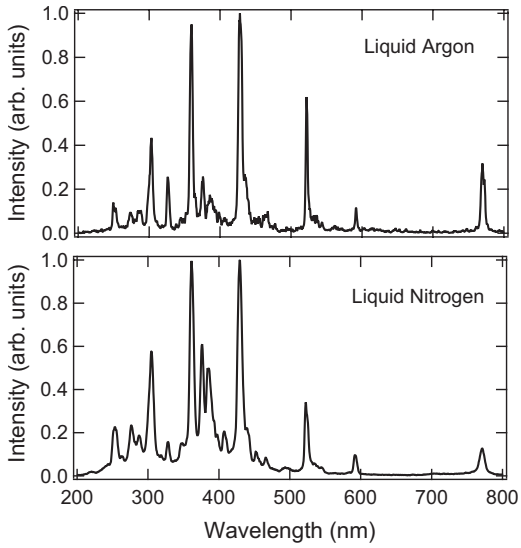

FIG. 7. Spectrum of the collapse luminescence in liquid nitrogen (T=66 K, p=4 bar) and liquid argon (T=84 K, p=4.5 bar).

lines of atomic argon or nitrogen, and that the spectral lines were exactly identical in the two different liquids. By increasing the resolution of the spectrometer it was found that two of the most prominent lines, at 358 and 428 nm, were actually triplet structures, as shown in Fig. 8 for the triplet at 428 nm. This enabled identification of these lines as coming from excited states of the chromium atom. We believe that the lines originate with microscopic flakes of stainless steel floating in the cryogenic liquids, probably knocked off the walls of the stainless cell by the intense shock wave generated by the initial laser ionization. The conducting flakes will then preferentially act to nucleate the ionization spot, and the expanding bubble will contain the vaporized chromium atoms (as well as all of the other components of stainless steel). We found by leaving the cell filled with liquid overnight that the collapse luminescence would not be visible the next morning until 50–100 shots of the laser were fired, and then it would begin appearing on every shot. Apparently the

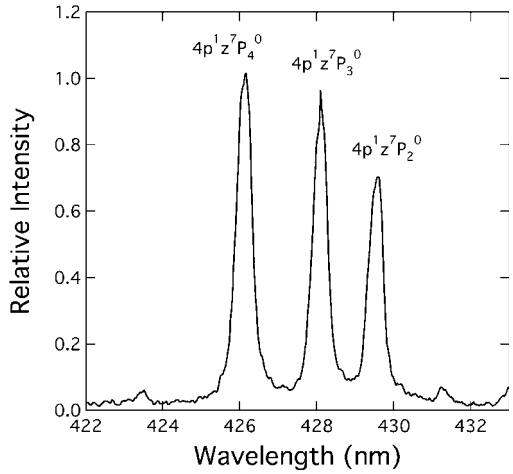

FIG. 8. Higher-resolution spectra of the chromium triplet lines around 428 nm in liquid nitrogen, showing the excited-state atomic configurations.

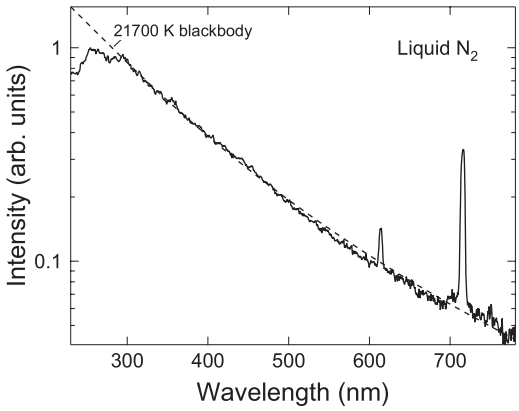

FIG. 9. Spectrum of the initial laser ionization in liquid nitrogen at T=66.0 K. The dashed curve shows the best fit to a blackbody spectrum.

flakes settled to the lower part of the cell until the liquid was stirred up by the heating and bubble generation of the laser. We surmise from this observation that the presence of the metallic atoms in the bubbles is necessary for the emission of a luminescence pulse. The presence of only nitrogen or argon vapor does not appear to give rise to any visible luminescence.

The temperatures in the interior of the bubble can be estimated from the relative intensities of the triplet chromium lines at 358 and 428 nm (Fig. 8). A similar estimate using chromium spectra has previously been used to find the temperatures in multibubble sonoluminescence [17]. By taking into account the degeneracies of each level, the relative intensities yield a temperature estimate of 4500 K. Though this is smaller than the water-bubble temperatures of order 8000 K, it is still remarkable considering that the starting temperature is 4 to 5 times lower than the water case. Since the ionization energy of chromium is 6.77 eV the degree of ionization should still be comparable to the case in water, where the smallest ionization energy, hydrogen, is 13.6 eV.

The fact that the spectra above consist entirely of discrete atomic lines suggests that the plasma being formed at the bubble collapse point has a relatively low electron density, as compared to the plasmas created in collapsing water bubbles which yield smooth blackbody spectra [4,7]. To study the question of how the spectrum evolves as a function of density we undertook spectral studies of the light emitted from the similar-sized plasma created by the initial laser ionization. Figure 9 shows the spectrum of the initial ionization pulse in liquid nitrogen. In the range from 300 to 650 nm this fits very well to a blackbody spectrum at a temperature of 21 700 K, showing that this plasma is optically thick, very similar to that observed for the ionization pulse in water [4]. The sharp features in this plot at 611 and 712 nm are not atomic line emission, but come from stimulated Raman scattering of the incident laser pulse. A substantial fraction of the beam at 1064 nm is upshifted to these wavelengths as it passes through the nitrogen, and is then scattered by the ionization plasma into the spectrometer.

The spectra of the ionization pulse in both liquid argon at 84 K and argon gas in the cell at room temperature is shown in Fig. 10. At low gas pressure the argon atomic lines are

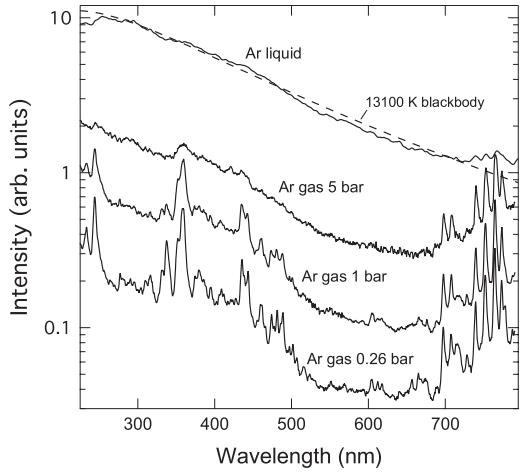

FIG. 10. Spectrum of the laser ionization in liquid argon at 84 K and argon gas at room temperature. The dashed curve shows the best fit to a blackbody spectrum.

clearly visible on top of a continuum component that rises into the ultraviolet. With increasing pressure the lines become both broadened and more difficult to see above the continuum, indicating that the plasma density is increasing as expected. The spectrum in liquid argon is mainly the smooth continuum, although the strong lines in the infrared are still visible. The continuum can be fit to a blackbody curve at 13 100 K over the region from 300 to 650 nm, shown as the dashed curve. There are no Raman lines here since the Raman gain for the 1064 nm laser in argon is much smaller than in nitrogen.

Figure 11 shows the spectra of the ionization pulse for hydrogen gas at room temperature. Similar to the argon case, the hydrogen lines broaden and become less visible compared to the continuum component. Of particular interest here is the hydrogen α line at 656.2 nm. The broadening of this line is known to depend primarily on the linear Stark effect [15]. The half-width of the line is proportional to the electric field in the plasma, and hence is found to vary with the electron density n_e as $\Delta\lambda = 0.04\, n_e^{2/3}$ nm, with the electron

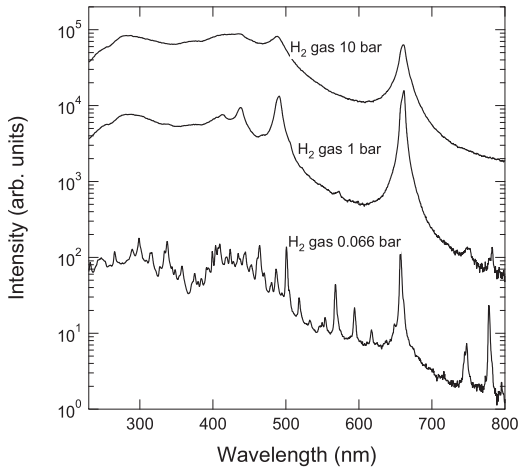

FIG. 11. Spectrum of the laser ionization in hydrogen gas at room temperature.

density in units of 10^{14} cm^{-3}. From the observed broadening we can then estimate the plasma densities as 3×10^{16} cm^{-3} in the 1 bar gas and 1×10^{17} in the 10 bar. These correspond to ionization fractions of 0.1% and 0.03%, respectively, for the two pressures.

IV. DISCUSSION

The slowly decaying metastable signal in Figs. 1 and 3 is similar to that seen in water [3] and results from the recombination products of the original laser ionization, and also from the excitation of the surrounding liquid by the photons emitted from the plasma, shown in Figs. 9 and 10. In liquid nitrogen, for example, there are a number of metastable atomic and molecular states that have lifetimes as large as 1 s even in the liquid environment, and which can be excited by blackbody illumination [16]. The observation of metastables affected by the bubble collapse as in Fig. 3 was a new feature that we have not seen previously for bubbles in water. The increasing density and temperature at the collapse point may quench the excited states inside the bubble nonradiatively, or there is also the possibility of photon emission outside of our detectable range of 200–800 nm. There also may be recombination reactions between the metastables as their density increases during the compression.

The need to pressurize the liquid to 3 to 4 bars before the collapse luminescence can be observed may be related to the thermal conduction apparent at the collapse point in Fig. 3(b). Large bubbles at 1 bar can take up to 200 μs to collapse, and the thermal losses may reduce the temperature in the interior during the collapse phase to such a degree that few photons are emitted. At higher pressures the collapse time, as given by Eq. (1), is considerably shorter, of order 50 μs at 4 bars. The more rapid collapse would then allow a higher final temperature and the onset of visible luminescence.

The large rebound of the bubble from the collapse point seen in Fig. 1 means that only a small fraction of the initial bubble energy has been lost in the collapse. In water bubbles it is known that quite a bit of the bubble energy is radiated away in the form of the acoustic shock wave generated by the large bubble-wall acceleration near the minimum radius. In liquid nitrogen this loss does not appear to be as strong, a sign that the bubble-wall motion does not change as rapidly. The unusually long pulse duration of the luminescence seen in Figs. 4 and 5 may be further evidence that the dynamics at the collapse point is slower. The heating of the gas in the bubble will depend primarily on the compression ratio of the maximum radius to the minimum, and appears to be roughly the same as for water, and reaches nearly the same temperatures. If the dynamics of the collapse point is say 100 times slower right at the collapse point, then the gas will stay hotter for a longer time, leading to a luminescence pulse 100 times longer as observed.

The physical reason for why the collapse dynamics could be so much slower than for water bubbles is unclear, however. The densities of liquid nitrogen and liquid argon are not so much different from water, and away from the collapse point the cryogenic bubbles appear to follow much the same

Rayleigh-Plesset dynamics that are known for water bubbles. The vapor pressures of the cryogenic liquids are 4 to 5 times larger than water at the temperatures we work at, and it is possible this could be a factor very close to the collapse point. The strong thermal conduction at the bubble wall visible in Fig. 2(b) could also possibly play a role in the dynamics. Unfortunately, even for the case of water bubbles there is no comprehensive theory for the duration of the luminescence pulse and the observed linear increase with maximum bubble size. The observation here of the same effect in cryogenic liquids, but with a duration 100 times longer, should provide a useful check for theories of the luminescence characteristics.

In further measurements with liquid nitrogen and argon it would be interesting to also measure the luminescence pulse width as a function of the applied pressure, something that we did not investigate. In water bubbles the width of the pulse increased as the pressure was increased [7], a result that is still not understood theoretically. The presence or absence of the same effect in cryogenic liquids would be useful data in gaining an understanding of the bubble dynamics in the neighborhood of the collapse point.

Another very speculative possibility is that the long pulse duration might not be associated with the bubble wall dynamics, but with the properties of the highly compressed material created at the collapse point. Since we know in this case that the luminescence originates from metallic atoms being compressed to solidlike densities at high pressure, this "pellet" may not immediately disintegrate when the bubble wall rebounds and the pressure is released. The formation of a metallic Fermi surface would give the pellet a relatively large heat capacity that could keep it glowing for an appreciable time past the collapse point.

We have not been able to conclusively identify all of the atomic lines in Fig. 7; higher-resolution studies will be necessary for this. In addition to the two strong triplet lines from chromium, one other line in Fig. 7 could be identified as coming from chromium, the line near 521 nm. Since the makeup of 304 stainless steel is about 70% iron, 18% chromium, 8% nickel, 2% manganese, 1% silicon, and much smaller amounts of carbon, phosphorus, and sulfur, we searched the NIST atomic database [18] for these elements to try to identify the other lines. Multiple lines from iron could account for the peaks near 250, 276, 287, 300, 376, and 386 nm, though there are some chromium lines that could also contribute to the 300 nm peak. The two lines in the red near 591 and 769 nm could not be identified as coming from any of the above elements. It is possible they could be the very strong lines from sodium and potassium at 589 and 766 nm, respectively, since the wavelength calibration of our spectrometer is not as reliable in the red, and the resolution degrades. The hot oxide anodization typically uses a solution of sodium and potassium nitrate, and though the cell was washed several times, some of this may still adhere to the surface of the particles. No lines from oxygen could be observed, which could have arisen either from the nitrates or from the surface iron oxide layer.

The reason that we could not observe any luminescence at all in liquid oxygen became clear once it was understood that the emission arose primarily from chromium and the other metallic atoms. Oxygen is much more reactive than nitrogen and argon, and it is known that the excited states of chromium and other metals are strongly quenched in the presence of oxygen [19]. The line emissions appear to be unaffected by argon and nitrogen atoms, which will certainly be present in the bubbles in those liquids due to the high vapor pressures. Since oxygen dissolves and mixes readily into liquid nitrogen, the quenching effect could be studied in greater detail by adding increasing amounts of oxygen and monitoring the changes in the collapse luminescence.

Although the characteristics of the luminescence indicate that the microscopic metal impurities floating in the cryogenic liquids are the source of the luminescence, one should really not think of these liquids as being "dirty." They are actually orders of magnitude cleaner than even high-purity water. The polar molecules of water attract and dissolve many substances, and water is filled with submicron impurites such as silicon flakes and organic protein fragments which are impossible to remove completely, even with repeated distillation and filtering. The cryogenic liquids are condensed from high-purity gases, and the only impurities will be the very low density of metallic flakes originating from the surface walls. We doubt that the anodization process was an appreciable factor in forming the impurities in our cell; similar impurity flakes are well-known to Raman spectroscopists using cryogenic liquids in stainless cells without anodization [20].

In any case, the presence of impurities is an absolute necessity for the laser-induced generation of bubbles to work at all in both water and the cryogenic liquids. The infrared absorption of these liquids is relatively small, and even a focused beam results in only mild local heating [such as seen in Fig. 2(b)] that is insufficient to generate a bubble. The $\sim$13 eV needed to ionize an atom of the pure liquid is much higher than the 1 eV photons in the laser beam; ionization would require a high order multiphoton absorption process that would be exceedingly unlikely to occur. The only process leading to bubble formation is nucleation of the laser absorption by an impurity. An impurity with a weakly bound electron can be easily ionized by the front of the laser pulse, and once there is free charge the energy absorption from the remainder of the laser pulse quickly leads to runaway ionization, and heating up to 20 000 K, as seen in Figs. 9 and 10 and Fig. 2 of Ref. [4].

The significant difference between the spectra observed in water and in the cryogenic liquids possibly results from a difference in the density of the atoms being compressed as the collapse point is approached. In water there is not enough time for recombination of the O and H atoms created in the initial dissociation of the laser hot spot. These atoms are different than the water molecules making up the bubble wall, and most are reflected from the wall, leaving a rather high density of O and H atoms inside the bubble at collapse, plus the much smaller number of impurity atoms from the nucleating impurity. The density of the resulting plasma is then apparently high enough to strongly absorb the emitted photons, such that a broadband spectrum of the luminescence is created [4]. In a cryogenic liquid such as argon, the vaporized atoms are argon atoms, and most of these will simply condense back into the liquid when they hit the bubble wall.

This then leaves mainly the impurity atoms to be heated and ionized at the collapse point, giving rise to a low-density plasma whose emission spectrum consists of atomic lines, like those seen in the low-density limits of Figs. 10 and 11. We have no doubt that among the many impurities floating in our water samples there must be a few stainless flakes from the cell walls. Occasionally these might be the nucleating impurities for the laser bubbles, but even if present in the collapsing bubbles the chromium emissions would be absorbed by the higher-density plasma, reemitted as part of the broadband spectrum, and hence would not be detectable.

V. CONCLUSIONS

In summary, we have observed luminescence at the collapse point of laser-created bubbles in liquid nitrogen and liquid argon. The duration of the luminescence pulse is proportional to the maximum bubble radius, but is about 100 times longer than observed for a similar sized bubble in water, a sign that the bubble wall dynamics near the collapse point are considerably slower in the cryogenic liquids than in water. The spectrum of the luminescence consists almost solely of atomic lines from neutral metallic atoms. It appears that this arises from microscopic flakes of stainless steel dislodged from the cell walls by the acoustic shock wave coming from the focused laser pulse; the floating flakes are then preferentially ionized by the laser, resulting in a substantial population of chromium and iron atoms in the interior of the bubble. As the bubble subsequently collapses, the atoms are heated by the rapid compression to temperatures of about 4500 K, giving rise to the light emission.

We speculate that it may be possible in further work with cryogenic fluids to eliminate the stainless flakes and hence the collapse luminescence, either by employing an all-glass cell, or by using materials other than stainless steel for the cell walls. Copper, for example, can be easily electropolished to minimize any hanging flakes, and since it is much softer than stainless steel the acoustic shock waves may not be able to dislodge the flakes. If it is possible to eliminate the flakes, it would then be interesting to add back powdered materials of a known size and composition. As the size of the powder flakes is increased the atomic density of the material in the resulting bubbles would be increased, and it might be possible to investigate the crossover from purely atomic lines seen in Fig. 7 to the smoother blackbodylike curves of Ref. [4], the process illustrated in Figs. 10 and 11. Though larger particles may not readily float, it may be possible to use ultrasonic agitation and/or levitation to get the particles into proximity with the laser beam. The ability to "tune" the plasma density at the collapse point could be quite useful in gaining an understanding of the details of the light-emission process.

ACKNOWLEDGMENT

This work was supported by the National Science Foundation, Grants No. DMR 01-31111 and No. 05-48521.

[1] M. Brenner, S. Hilgenfeldt, and D. Lohse, Rev. Mod. Phys. **74**, 425 (2002).
[2] C. D. Ohl, O. Lindau, and W. Lauterborn, Phys. Rev. Lett. **80**, 393 (1998).
[3] O. Baghdassarian, B. Tabbert, and G. A. Williams, Phys. Rev. Lett. **83**, 2437 (1999).
[4] O. Baghdassarian, H.-C. Chu, B. Tabbert, and G. A. Williams, Phys. Rev. Lett. **86**, 4934 (2001).
[5] K. R. Weninger, C. G. Camara, and S. J. Putterman, Phys. Rev. Lett. **83**, 2081 (1999).
[6] A. Chakravarty, T. Georghiou, T. E. Phillipson, and A. J. Walton, Phys. Rev. E **69**, 066317 (2004).
[7] E. A. Brujan, D. S. Hecht, F. Lee, and G. A. Williams, Phys. Rev. E **72**, 066310 (2005).
[8] P. Jarman and K. Taylor, J. Low Temp. Phys. **2**, 389 (1970).
[9] P. I. Golubnichii, V. D. Goncharov, and Kh. V. Protopopov, Sov. Phys. Acoust. **16**, 323 (1971).
[10] M. Bernard, M. Fauver, and G. A. Williams, Physica B **194-196**, 165 (1994).
[11] O. Baghdassarian, H. Cho, E. Varoquaux, and G. A. Williams, J. Low Temp. Phys. **110**, 305 (1998).
[12] M. Tsubota, Y. Tomita, A. Shima, and I. Kano, JSME Int. J., Ser. B **39**, 257 (1996).
[13] O. Baghdassarian, B. Tabbert, and G. A. Williams, Physica B **284-288**, 393 (2000); *Proceedings of CAV2001*, edited by C. E. Brennen, S. L. Ceccio, and R. E. A. Arndt, http://cav2001.library.caltech.edu/archive/00000324
[14] Cryo Industries of America, Inc., Manchester, NH.
[15] I. H. Hutchinson, *Principles of Plasma Diagnostics* (Cambridge University Press, New York, 1978).
[16] D. Chandler and G. Ewing, J. Chem. Phys. **73**, 4904 (1980).
[17] W. B. McNamara, Y. T. Didenko, and K. S. Suslick, Nature (London) **401**, 772 (1999).
[18] NIST Atomic Spectra Database, http://physics.nist.gov/PhysRefData/ASD/index.html
[19] K. Honma, J. Phys. Chem. A **103**, 1809 (1999).
[20] *Molecular Cryospectroscopy*, edited by R. J. H. Clark and R. E. Hester (Wiley, New York, 1995).